

Light-front quark model analysis of heavy meson radiative decays

Ho-Meoyng Choi

Department of Physics, Teachers College, Kyungpook National University, Daegu, Korea 702-701

We present the magnetic dipole($M1$) transitions $V \rightarrow P\gamma$ of various heavy-flavored mesons such as $(D, D^*, D_s, D_s^*, \eta_c, J/\psi)$ and $(B, B^*, B_s, B_s^*, \eta_b, \Upsilon)$ using the light-front quark model constrained by the variational principle for the QCD-motivated effective Hamiltonian. The weak decay constants of heavy mesons and the decay widths for $V \rightarrow P\gamma$ are calculated. The radiative decay for $\Upsilon \rightarrow \eta_b\gamma$ process is found to be very helpful to determine the unmeasured mass of η_b . Our numerical results are overall in good agreement with the available experimental data as well as other theoretical model calculations.

I. INTRODUCTION

The physics of exclusive heavy meson decays has provided very useful testing ground for the precise determination of the fundamental parameters of the standard model(SM) and the development of a better understanding of the QCD dynamics. While the experimental tests of exclusive heavy meson decays are much easier than those of inclusive one, the theoretical understanding of exclusive decays is complicated mainly due to the nonperturbative hadronic matrix elements entered in the long distance nonperturbative contributions. Since a rigorous field-theoretic formulation with a first principle application of QCD to make a reliable estimates of the nonperturbative hadronic matrix elements has not so far been possible, most of theoretical efforts have been devoted to looking for phenomenological approaches to nonperturbative QCD dynamics.

In our previous light-front quark model(LFQM) analysis [1] based on the QCD-motivated effective Hamiltonian, we have analyzed various exclusive processes such as the semileptonic decays between heavy pseudoscalar mesons [2] and the rare $B \rightarrow K$ decays [3] and found a good agreement with the experimental data. Along with those exclusive processes, the magnetic dipole($M1$) transitions $V(1^3S_1) \rightarrow P(1^1S_0)\gamma$ from the spin-triplet S -wave vector(V) mesons to the spin-singlet S -wave pseudoscalar(P) mesons have also been considered as a valuable testing ground to further constrain the phenomenological model of hadrons [4, 5, 6, 7, 8, 9, 10, 11, 12, 13].

In this talk we thus investigate the magnetic dipole transition among the heavy-flavored mesons such as $(D, D^*, D_s, D_s^*, \eta_c, J/\psi)$ and $(B, B^*, B_s, B_s^*, \eta_b, \Upsilon)$ using our LFQM [1, 2, 3]. Since the experimental data available in this heavy-flavored sector are scanty, predictions of a model, if found reliable, can be utilized quite fruitfully. In addition, we calculate the weak decay constants of heavy pseudoscalar and vector mesons. A reliable estimate of decay constants is important, as they appear in many processes from which we can extract fundamental quantities in the SM such as Cabibbo-Kobayashi-Maskawa matrix elements. In our LFQM [1, 2, 3], we have implemented the variational principle to QCD-motivated effective LF Hamiltonian to enable us to analyze the meson mass spectra and to find optimized model parameters, which

are to be used subsequently in the present investigation. Such an approach can better constrain the phenomenological parameters and establish the extent of applicability of our LFQM to wider ranging hadronic phenomena.

The paper is organized as follows: In Sec.II, we briefly describe the formulation of our LFQM [1, 2] and the procedure of fixing the model parameters using the variational principle for the QCD-motivated effective Hamiltonian. The decay constants and radiative $V \rightarrow P\gamma$ decay widths for heavy-flavored mesons are then uniquely determined in our model calculation. In Sec. III, the formulae for the decay constants of pseudoscalar and vector mesons as well as the decay widths for $V \rightarrow P\gamma$ in our LFQM are given. To obtain the q^2 -dependent transition form factors $F_{VP}(q^2)$ for $V \rightarrow P\gamma^*$ transitions, we use the Drell-Yan-West $q^+ = 0$ frame(i.e. $q^2 = -\mathbf{q}_\perp^2 < 0$) and then analytically continue the spacelike results to the timelike $q^2 > 0$ region by changing \mathbf{q}_\perp to $i\mathbf{q}_\perp$ in the form factor. The coupling constants $g_{VP\gamma}$ needed for the calculations of the decay widths for $V \rightarrow P\gamma$ can then be determined in the limit as $q^2 \rightarrow 0$, i.e. $g_{VP\gamma} = F_{VP}(q^2 = 0)$. In Sec. IV, we present our numerical results and compare with the available experimental data as well as other theoretical model predictions. Summary and conclusions follow in Sec.V.

II. MODEL DESCRIPTION

The key idea in our LFQM [1, 2] for mesons is to treat the radial wave function as trial function for the variational principle to the QCD-motivated effective Hamiltonian saturating the Fock state expansion by the constituent quark and antiquark. The QCD-motivated Hamiltonian for a description of the ground state meson mass spectra is given by

$$\begin{aligned} H_{q\bar{q}}|\Psi_{nlm}^{JJ_z}\rangle &= \left[\sqrt{m_q^2 + \vec{k}^2} + \sqrt{m_{\bar{q}}^2 + \vec{k}^2} + V_{q\bar{q}} \right] |\Psi_{nlm}^{JJ_z}\rangle, \\ &= [H_0 + V_{q\bar{q}}]|\Psi_{nlm}^{JJ_z}\rangle = M_{q\bar{q}}|\Psi_{nlm}^{JJ_z}\rangle, \end{aligned} \quad (1)$$

where $\vec{k} = (\mathbf{k}_\perp, k_z)$ is the three-momentum of the constituent quark, $M_{q\bar{q}}$ is the mass of the meson, and $|\Psi_{nlm}^{JJ_z}\rangle$ is the meson wave function. In this work, we use two interaction potentials $V_{q\bar{q}}$ for the pseudoscalar(0^{-+}) and

vector(1^{--}) mesons: (1) Coulomb plus harmonic oscillator(HO), and (2) Coulomb plus linear confining potentials. In addition, the hyperfine interaction, which is essential to distinguish vector from pseudoscalar mesons, is included for both cases, viz.,

$$V_{q\bar{q}} = V_0 + V_{\text{hyp}} = a + \mathcal{V}_{\text{conf}} - \frac{4\alpha_s}{3r} + \frac{2}{3} \frac{\mathbf{S}_q \cdot \mathbf{S}_{\bar{q}}}{m_q m_{\bar{q}}} \nabla^2 V_{\text{coul}}, \quad (2)$$

where $\mathcal{V}_{\text{conf}} = br(r^2)$ for the linear(HO) potential and $\langle \mathbf{S}_q \cdot \mathbf{S}_{\bar{q}} \rangle = 1/4(-3/4)$ for the vector(pseudoscalar) meson.

The momentum space light-front wave function of the ground state pseudoscalar and vector mesons is given by

$$\Psi_{100}^{JJ_z}(x_i, \mathbf{k}_{i\perp}, \lambda_i) = \mathcal{R}_{\lambda_1 \lambda_2}^{JJ_z}(x_i, \mathbf{k}_{i\perp}) \phi(x_i, \mathbf{k}_{i\perp}), \quad (3)$$

where $\phi(x_i, \mathbf{k}_{i\perp})$ is the radial wave function and $\mathcal{R}_{\lambda_1 \lambda_2}^{JJ_z}$ is the spin-orbit wave function, which is obtained by the interaction independent Melosh transformation from the ordinary equal-time static spin-orbit wave function assigned by the quantum numbers J^{PC} . The model wave function in Eq. (3) is represented by the Lorentz-invariant variables, $x_i = p_i^+ / P^+$, $\mathbf{k}_{i\perp} = \mathbf{p}_{i\perp} - x_i \mathbf{P}_{\perp}$ and λ_i , where $P^\mu = (P^+, P^-, \mathbf{P}_{\perp}) = (P^0 + P^3, (M^2 + \mathbf{P}_{\perp}^2) / P^+, \mathbf{P}_{\perp})$ is the momentum of the meson M , p_i^μ and λ_i are the momenta and the helicities of constituent quarks, respectively.

The covariant forms of the spin-orbit wave functions for pseudoscalar and vector mesons are given by

$$\begin{aligned} \mathcal{R}_{\lambda_1 \lambda_2}^{00} &= \frac{-\bar{u}(p_1, \lambda_1) \gamma_5 v(p_2, \lambda_2)}{\sqrt{2} \tilde{M}_0}, \\ \mathcal{R}_{\lambda_1 \lambda_2}^{1J_z} &= \frac{-\bar{u}(p_1, \lambda_1) \left[\not{\epsilon}(J_z) - \frac{\epsilon \cdot (p_1 - p_2)}{M_0 + m_1 + m_2} \right] v(p_2, \lambda_2)}{\sqrt{2} \tilde{M}_0}, \end{aligned} \quad (4)$$

where $\epsilon^\mu(J_z)$ is the polarization vector of the vector meson [14], $\tilde{M}_0 = \sqrt{M_0^2 - (m_1 - m_2)^2}$ and M_0^2 is the invariant meson mass square M_0^2 defined as $M_0^2 = \sum_{i=1}^2 \frac{\mathbf{k}_{i\perp}^2 + m_i^2}{x_i}$. The spin-orbit wave functions satisfy the following relations $\sum_{\lambda_1 \lambda_2} \mathcal{R}_{\lambda_1 \lambda_2}^{JJ_z \dagger} \mathcal{R}_{\lambda_1 \lambda_2}^{JJ_z} = 1$, for both pseudoscalar and vector mesons. For the radial wave function ϕ , we use the same Gaussian wave function for both pseudoscalar and vector mesons

$$\phi(x_i, \mathbf{k}_{i\perp}) = \frac{4\pi^{3/4}}{\beta^{3/2}} \sqrt{\frac{\partial k_z}{\partial x}} \exp(-\vec{k}^2 / 2\beta^2), \quad (5)$$

where β is the variational parameter. When the longitudinal component k_z is defined by $k_z = (x - 1/2)M_0 + (m_2^2 - m_1^2) / 2M_0$, the Jacobian of the variable transformation $\{x, \mathbf{k}_{\perp}\} \rightarrow \vec{k} = (\mathbf{k}_{\perp}, k_z)$ is given by

$$\frac{\partial k_z}{\partial x} = \frac{M_0}{4x_1 x_2} \left\{ 1 - \left[\frac{m_1^2 - m_2^2}{M_0^2} \right]^2 \right\}. \quad (6)$$

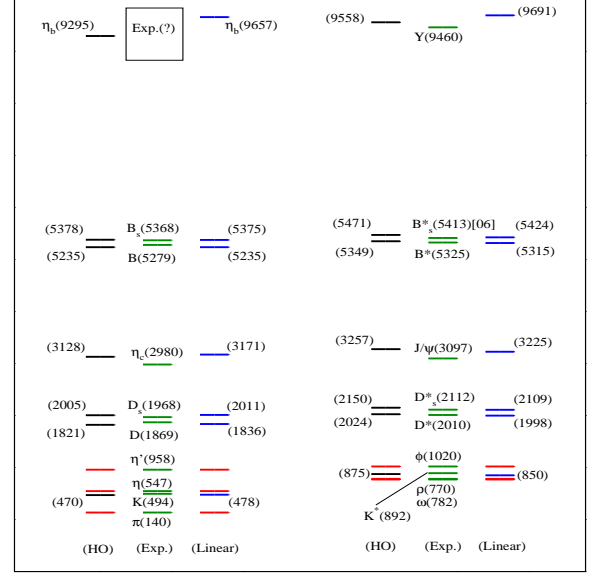


FIG. 1: (Color online). Fit of the ground state meson masses[MeV] with the parameters given in Table I. The (ρ, π) , (η, η') , and (ω, ϕ) masses are our input data(red online).

The normalization factor in Eq. (5) is obtained from the following normalization of the total wave function,

$$\int_0^1 dx \int \frac{d^2 \mathbf{k}_{\perp}}{16\pi^3} |\Psi_{100}^{JJ_z}(x, \mathbf{k}_{i\perp})|^2 = 1. \quad (7)$$

Our variational principle to the QCD-motivated effective Hamiltonian first evaluate the expectation value of the central Hamiltonian $H_0 + V_0$, i.e. $\langle \phi | (H_0 + V_0) | \phi \rangle$ with a trial function $\phi(x_i, \mathbf{k}_{i\perp})$ that depends on the variational parameters β and varies β until $\langle \phi | (H_0 + V_0) | \phi \rangle$ is a minimum. Once these model parameters are fixed, then, the mass eigenvalue of each meson is obtained by $M_{q\bar{q}} = \langle \phi | (H_0 + V_{q\bar{q}}) | \phi \rangle$. More detailed procedure of determining the model parameters of light and heavy quark sectors can be found in our previous works [1, 2]. Our model parameters (m, β) for the heavy quark sector obtained from the linear and HO potential models are summarized in Table I.

Our predictions of the ground state meson mass spectra obtained from the linear and HO potential parameters are summarized in Fig. 1. As one can see, our predictions obtained from both linear and HO parameters are overall in good agreement with the data [15] within 6% error. As we shall see in our numerical calculations, the radiative decay of $\Upsilon \rightarrow \eta_b \gamma$ might be useful to determine the mass of η_b experimentally since the decay width $\Gamma(\Upsilon \rightarrow \eta_b \gamma)$ is very sensitive to the value of $\Delta m (= M_{\Upsilon} - M_{\eta_b})$, viz. $\Gamma \propto (\Delta m)^3$.

The decay constants of pseudoscalar and vector mesons

TABLE I: The constituent quark mass[GeV] and the Gaussian paramters β [GeV] for the linear and HO potentials obtained by the variational principle. $q = u$ and d .

Model	m_q	m_s	m_c	m_b	β_{qc}	β_{sc}	β_{cc}	β_{qb}	β_{sb}	β_{bb}
Linear	0.22	0.45	1.8	5.2	0.468	0.502	0.651	0.527	0.571	1.145
HO	0.25	0.48	1.8	5.2	0.422	0.469	0.700	0.496	0.574	1.803

are defined by

$$\begin{aligned} \langle 0|\bar{q}\gamma^\mu\gamma_5q|P\rangle &= if_P P^\mu, \\ \langle 0|\bar{q}\gamma^\mu q|V(P, h)\rangle &= f_V M_V \epsilon^\mu(h), \end{aligned} \quad (8)$$

where the experimental value of vector meson decay constant f_V is extracted from the longitudinal($h = 0$) polarization. Using the plus component($\mu = +$) of the current, one can easily calculate the decay constants and the explicit forms of pseudoscalar and vector meson decay constants are given in [14].

III. RADIATIVE DECAY WIDTH FOR $V \rightarrow P\gamma$

In our LFQM calculation of $V \rightarrow P\gamma$ decay process, we shall first analyze the virtual photon(γ^*) decay process so that we calculate the momentum dependent transition form factor, $F_{VP}(q^2)$. The lowest-order Feynman diagram for $V \rightarrow P\gamma^*$ process is shown in Fig. 2 where the decay from vector meson to pseudoscalar meson and virtual photon state is mediated by a quark loop with flavors of constituent mass m_1 and m_2 .

The transition form factor $F_{VP}(q^2)$ for the magnetic dipole decay of vector meson $V(P) \rightarrow P(P')\gamma^*(q)$ is defined as

$$\langle P(P')|J_{\text{em}}^\mu|V(P, h)\rangle = ie\epsilon^{\mu\nu\rho\sigma}\epsilon_\nu(P, h)q_\rho P_\sigma F_{VP}(q^2), \quad (9)$$

where $q = P - P'$ is the four momentum of the virtual photon, $\epsilon_\nu(P, h)$ is the polarization vector of the initial meson with four momentum P and helicity h . The kinematically allowed momentum transfer squared q^2 ranges from 0 to $q_{\text{max}}^2 = (M_V - M_P)^2$.

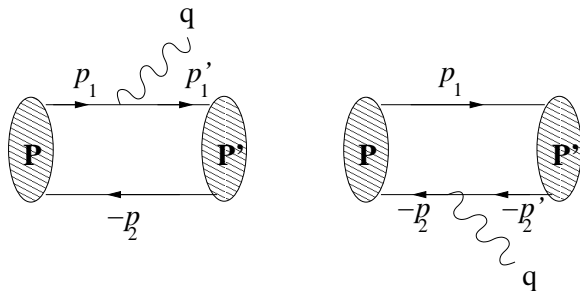


FIG. 2: Lowest-order graph for $V \rightarrow P\gamma^*$ transitions.

The decay form factor $F_{VP}(q^2)$ can be obtained in the $q^+ = 0$ frame with the “good” component of currents, i.e. $\mu = +$, without encountering zero-mode contributions [16]. Thus, we shall perform our LFQM calculation in the $q^+ = 0$ frame, where $q^2 = q^+q^- - \mathbf{q}_\perp^2 = -\mathbf{q}_\perp^2 < 0$, and then analytically continue the form factor $F_{VP}(\mathbf{q}_\perp^2)$ in the spacelike region to the timelike $q^2 > 0$ region by changing \mathbf{q}_\perp to $i\mathbf{q}_\perp$ in the form factor. In the calculations of the decay form factor $F_{VP}(q^2)$, we use ‘+’-component of currents and the transverse($h = \pm 1$) polarization.

The hadronic matrix element of the plus current, $\langle J^+ \rangle \equiv \langle P(P')|J_{\text{em}}^+|V(P, h = +)\rangle$ in Eq. (9) is then obtained by the convolution formula of the initial and final state light-front wave functions:

$$\begin{aligned} \langle J^+ \rangle &= \sum_j ee_j \int_0^1 \frac{dx}{16\pi^3} \int d^2\mathbf{k}_\perp \phi(x, \mathbf{k}'_\perp) \phi(x, \mathbf{k}_\perp) \\ &\times \sum_{\lambda\bar{\lambda}} \mathcal{R}_{\lambda'\bar{\lambda}}^{00\dagger} \frac{\bar{u}_{\lambda'}(p'_1)}{\sqrt{p_1'^+}} \gamma^+ \frac{u_\lambda(p_1)}{\sqrt{p_1^+}} \mathcal{R}_{\lambda\bar{\lambda}}^{11}, \end{aligned} \quad (10)$$

where $\mathbf{k}'_\perp = \mathbf{k}_\perp - x_2\mathbf{q}_\perp$ and ee_j is the electrical charge for j -th quark flavor. Comparing with the right-hand-side of Eq. (9), i.e. $eP^+F_{VP}(Q^2)q^R/\sqrt{2}$ where $q^R = q_x + iq_y$, we could extract the one-loop integral, $I(m_1, m_2, q^2)$, which is given by

$$\begin{aligned} I(m_1, m_2, q^2) &= \int_0^1 \frac{dx}{8\pi^3} \int d^2\mathbf{k}_\perp \frac{\phi(x, \mathbf{k}'_\perp) \phi(x, \mathbf{k}_\perp)}{x_1 \tilde{M}_0 \tilde{M}'_0} \\ &\times \left\{ \mathcal{A} + \frac{2}{\mathcal{M}_0} \left[\mathbf{k}_\perp^2 - \frac{(\mathbf{k}_\perp \cdot \mathbf{q}_\perp)^2}{\mathbf{q}_\perp^2} \right] \right\}, \end{aligned} \quad (11)$$

where the primed factors are the functions of final state momenta, e.g. $\tilde{M}'_0 = \tilde{M}'_0(x, \mathbf{k}'_\perp)$.

Then, the decay form factor $F_{VP}(q^2)$ is obtained as

$$F_{VP}(q^2) = e_1 I(m_1, m_2, q^2) + e_2 I(m_2, m_1, q^2). \quad (12)$$

The coupling constant $g_{VP\gamma}$ for real photon(γ) case can then be determined in the limit as $q^2 \rightarrow 0$, i.e. $g_{VP\gamma} = F_{VP}(q^2 = 0)$. The decay width for $V \rightarrow P\gamma$ is given by

$$\Gamma(V \rightarrow P\gamma) = \frac{\alpha}{3} g_{VP\gamma}^2 k_\gamma^3, \quad (13)$$

where α is the fine-structure constant and $k_\gamma = (M_V^2 - M_P^2)/2M_V$ is the kinematically allowed energy of the outgoing photon.

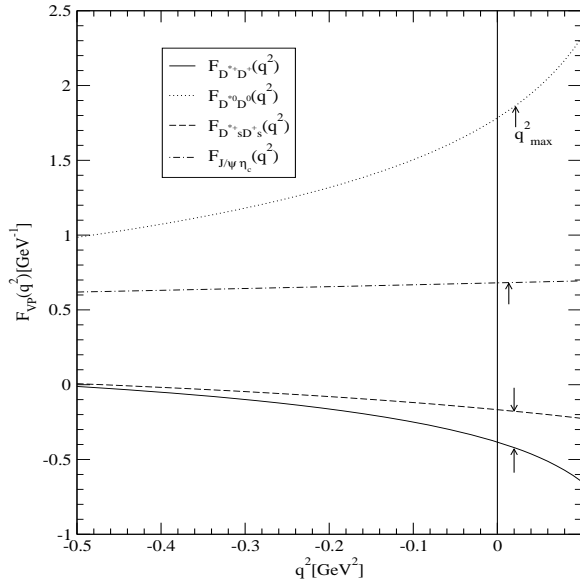


FIG. 3: Transition form factors $F_{VP}(q^2)$ for charmed mesons radiative decays obtained from the linear parameters.

IV. NUMERICAL RESULTS

In our numerical calculations, we use two sets of model parameters (m, β) for the linear and HO confining potentials given in Table I to perform, in a way, a parameter-free-calculation of decay constants and decay rates for heavy pseudoscalar and vector mesons. Although our predictions of ground state heavy meson masses are overall in good agreement with the experimental values, we use the experimental meson masses except η_b meson in the computations of the radiative decay widths to reduce possible theoretical uncertainties. Since the η_b mass is not measured yet, we use the range $\Delta m = M_\Upsilon - M_{\eta_b} = 60 \sim 160$ MeV for $\Upsilon \rightarrow \eta_b \gamma$ process [17].

In Tables II and III, we present our predictions for the charmed and bottomed meson decay constants, respectively, and compare them with other theoretical model predictions [18, 19, 20, 21, 22, 23, 24, 25, 26] as well as the experimental data [15, 27, 28, 29, 30]. Our predictions for the ratios $f_{D_s}/f_D = 1.18[1.20]$ and $f_{\eta_c}/f_{J/\psi} = 0.91[0.90]$ obtained from the linear[HO] parameters are in good agreement with the available experimental data, $(f_{D_s}/f_D)_{\text{exp.}} = 1.23 \pm 0.11 \pm 0.04$ [28] and $(f_{\eta_c}/f_{J/\psi})_{\text{exp.}} = 0.81 \pm 0.19$ [15, 29], respectively. Our results for the ratios $f_{B_s}/f_B = 1.24[1.32]$ and $f_{B_s^*}/f_{B^*} = 1.23[1.32]$ obtained from the linear[HO] parameters are quite comparable with the recent lattice results, $1.20(3)(1)$ [24] and $1.22(_{-6}^{+5})$ [25] for $f_{B_s^*}/f_{B^*}$ and $1.17(4)_{-3}^{+1}$ [18] for $f_{B_s^*}/f_{B^*}$.

We show in Fig. 3 the momentum dependent form factors $F_{VP}(q^2)$ for charmed vector meson radiative $V \rightarrow P\gamma^*$ decays obtained from the linear parameters. Since

the results from the HO parameters are not much different from those of linear ones, we omit them for simplicity. The arrows in the figure represent the zero recoil points of the final state pseudoscalar meson, i.e. $q^2 = q_{\text{max}}^2$. We have performed the analytical continuation of the decay form factors $F_{VP}(q^2)$ from the spacelike region ($q^2 < 0$) to the physical timelike region $0 \leq q^2 \leq q_{\text{max}}^2$. The coupling constant $g_{VP\gamma}$ at $q^2 = 0$ corresponds to a final state pseudoscalar meson recoiling with maximum three-momentum in the rest frame of vector meson. The opposite sign of coupling constants for D^{*+} (solid line) and D_s^{*+} (dashed line) decays compared to the charmonium J/ψ (dot-dashed line) decay indicates that the charmed quark contribution is largely destructive in the radiative decays of D^{*+} and D_s^{*+} mesons. The recoil effect, i.e. the difference between the zero and the maximum points, is not negligible for the $D^{*+} \rightarrow D^+\gamma^*$ decay, while other processes may be negligible. The recoil effects for the bottomed and bottomonium meson decays are negligible due to the very small photon energies.

In Table IV, we present our results for the decay widths and branching ratios together with the available experimental data. The errors in our results for the decay widths and branching ratios come from the uncertainties of the experimental mass values and experimental mass values plus the full widths, respectively. Our results of the branching ratios $\text{Br}(J/\psi \rightarrow \eta_c \gamma) = 1.80 \pm 0.10[1.76 \pm 0.10]\%$ and $\text{Br}(D^* \rightarrow D^+\gamma) = 0.93 \pm 0.31[1.00 \pm 0.34]\%$ obtained from the linear[HO] parameters are in agreement with the experimental data [15], $\text{Br}(J/\psi \rightarrow \eta_c \gamma)_{\text{exp}} = (1.3 \pm 0.4)\%$ and $\text{Br}(D^* \rightarrow D^+\gamma)_{\text{exp}} = (1.6 \pm 0.4)\%$ within the error bars. For the $\Upsilon \rightarrow \eta_b \gamma$ process, our predictions for the decay width and branching ratio obtained from the linear[HO] parameters are $\Gamma(\Upsilon \rightarrow \eta_b \gamma) = 45_{-38}^{+97}[42_{-36}^{+88}]$ eV and $\text{Br}(\Upsilon \rightarrow \eta_b \gamma) = (8.4_{-7.2}^{+18.6})[7.7_{-6.6}^{+17.0}] \times 10^{-4}$, where the lower, central, and upper values correspond to $\Delta m = 60$ MeV, 110 MeV, and 160 MeV, respectively. The decay width $\Gamma(\Upsilon \rightarrow \eta_b \gamma)$ is found to be very sensitive to Δm because it is proportional to $(\Delta m)^3$. Other model calculations for the $\Upsilon(1S)$ radiative $M1$ decay rates can be found in Ref. [31].

In Fig. 4, we show the dependence of $\Gamma(\Upsilon \rightarrow \eta_b \gamma)$ on Δm compared with other theoretical model calculations [32]. As one can see from Fig. 4, our prediction for the dependence of $\Gamma(\Upsilon \rightarrow \eta_b \gamma)$ on Δm is quite consistent with other theoretical predictions for various Δm [32].

V. SUMMARY AND DISCUSSION

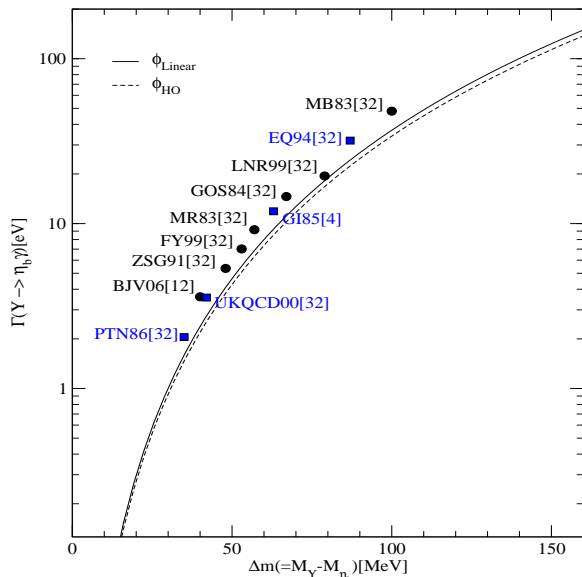
In this work, we investigated the weak decay constants and the magnetic dipole $V \rightarrow P\gamma$ decays of heavy-flavored mesons such as $(D, D^*, D_s, D_s^*, \eta_c, J/\psi)$ and $(B, B^*, B_s, B_s^*, \eta_b, \Upsilon)$ using the LFQM constrained by the variational principle for the QCD-motivated effective Hamiltonian. Our model parameters obtained from the variational principle uniquely determine the above

TABLE II: Charmed meson decay constants(in unit of MeV) obtained from the linear[HO] parameters.

	f_D	f_{D^*}	f_{D_s}	$f_{D_s^*}$	f_{η_c}	$f_{J/\psi}$
Linear[HO]	211[194]	254[228]	248[233]	290[268]	326[354]	360[395]
Lattice [18]	$211 \pm 14_{-12}^{+2}$	$245 \pm 20_{-2}^{+3}$	$231 \pm 12_{-1}^{+8}$	$272 \pm 16_{-20}^{+3}$	—	—
QCD [19]	$201 \pm 3 \pm 17$	—	$249 \pm 3 \pm 16$	-	—	—
Sum-rules [20]	204 ± 20	—	235 ± 24	-	—	—
BS [21]	230 ± 25	340 ± 23	248 ± 27	375 ± 24	292 ± 25	459 ± 28
QM [22]	240 ± 20	—	290 ± 20	—	—	—
RQM [23]	234	310	268	315	—	—
Exp.	$222.6 \pm 16.7_{-3.4}^{+2.8}$ [27]	—	$274 \pm 13 \pm 7$ [28]	-	335 ± 75 [29]	416 ± 6 [15]

TABLE III: Bottomed meson decay constants(in unit of MeV) obtained from the linear[HO] parameters.

	f_B	f_{B^*}	f_{B_s}	$f_{B_s^*}$	f_{η_b}	f_{Υ}
Linear[HO]	189[180]	204[193]	234[237]	250[254]	507[897]	529[983]
Lattice [18]	$179 \pm 18_{-9}^{+34}$	$196 \pm 24_{-2}^{+39}$	$204 \pm 16_{-0}^{+36}$	$229 \pm 20_{-16}^{+41}$	—	—
QCD [24]	216 ± 22	—	259 ± 32	—	—	—
[25]	189 ± 27	—	230 ± 30	-	—	—
Sum-rules [26]	210 ± 19	—	244 ± 21	-	—	—
[20]	203 ± 23	—	236 ± 30	-	—	—
BS [21]	196 ± 29	238 ± 18	216 ± 32	272 ± 20	—	498 ± 20
QM [22]	155 ± 15	—	210 ± 20	—	—	—
RQM [23]	189	219	218	251	—	—
Exp.	229_{-31-37}^{+36+34} [30]	—	—	-	—	715 ± 5 [15]

FIG. 4: The dependence of $\Gamma(\Upsilon \rightarrow \eta_b \gamma)$ on $\Delta m = M_\Upsilon - M_{\eta_b}$ compared with other theoretical model calculations [32].

nonperturbative quantities. This approach can establish the extent of applicability of our LFQM to wider ranging hadronic phenomena.

Our predictions of mass spectra and decay constants for heavy pseudoscalar and vector mesons are overall in

good agreement with the available experimental data as well as other theoretical model calculations. Our numerical results of the decay widths for $J/\psi \rightarrow \eta_c \gamma$ and $D^{*+} \rightarrow D^+ \gamma$ fall within the experimental error bars. Our predictions for the branching ratios for the bottomed and bottomed-strange mesons are quite comparable with other theoretical model predictions. For the radiative decay of the bottomonium, we find that the decay widths $\Gamma(\Upsilon \rightarrow \eta_b \gamma)$ is very sensitive to the value of $\Delta m = M_\Upsilon - M_{\eta_b}$. This sensitivity for the bottomonium radiative decay may help to determine the mass of η_b experimentally.

Since the form factor $F_{VP}(q^2)$ of vector meson radiative decay $V \rightarrow P\gamma^*$ presented in this work is precisely analogous to the vector current form factor $g(q^2)$ in weak decay of ground state pseudoscalar meson to ground state vector meson, the ability of our model to describe such decay is therefore relevant to the reliability of the model for the weak decay. Consideration on such exclusive weak decays in our LFQM is underway. Although our previous LFQM [1, 2] and this analyses did not include the heavy mesons comprising both c and b quarks such as B_c and B_c^* , the extension of our LFQM to these mesons will be explored in our future communication.

Acknowledgments

This work was supported by a grant from Korea Research Foundation under the contract KRF-2005-070-C00039.

TABLE IV: Decay widths and branching ratios for radiative $V \rightarrow P\gamma$ decays obtained from our linear[HO] model parameters. We used $M_{\eta_b} = 9353 \pm 50$ MeV for $\Upsilon \rightarrow \eta_b\gamma$ decay.

Decay mode	Γ [keV]	Br	Br_{exp} [15]
$J/\psi \rightarrow \eta_c\gamma$	1.69 ± 0.05 [1.65 ± 0.05]	(1.80 ± 0.10) [1.76 ± 0.10]	$(1.3 \pm 0.4)\%$
$D^{*+} \rightarrow D^+\gamma$	0.90 ± 0.02 [0.96 ± 0.02]	(0.93 ± 0.31) [1.00 ± 0.34]	$(1.6 \pm 0.4)\%$
$D^{*0} \rightarrow D^0\gamma$	20.0 ± 0.3 [21.0 ± 0.3]	-	$(38.1 \pm 2.9)\%$
$D_s^{*+} \rightarrow D_s^+\gamma$	0.18 ± 0.01 [0.17 ± 0.01]	-	$(94.2 \pm 0.7)\%$
$B^{*+} \rightarrow B^+\gamma$	0.40 ± 0.03 [0.40 ± 0.03]	-	-
$B^{*0} \rightarrow B^0\gamma$	0.13 ± 0.01 [0.13 ± 0.01]	-	-
$B_s^{*0} \rightarrow B_s^0\gamma$	0.068 ± 0.017 [0.064 ± 0.016]	-	-
$\Upsilon \rightarrow \eta_b\gamma$	$0.045_{-0.038}^{+0.097}$ [$0.042_{-0.036}^{+0.088}$]	$(8.4_{-7.2}^{+18.6})$ [$7.7_{-6.6}^{+17.0}$]	$\times 10^{-4}$

- [1] H.-M. Choi and C.-R. Ji, Phys. Rev. D **59**, 074015 (1999).
[2] H.-M. Choi and C.-R. Ji, Phys. Lett. B **460**, 461 (1999).
[3] H.-M. Choi, C.-R. Ji, and L.S. Kisslinger, Phys. Rev. D **65**, 074032 (2002).
[4] S. Godfrey and N. Isgur, Phys. Rev. D **32**, 189 (1985).
[5] N. Barik and P.C. Dash, Phys. Rev. D **49**, 299 (1994).
[6] W. Jaus, Phys. Rev. D **53**, 1349 (1996).
[7] D. Ebert, R.N. Faustov, and V.O. Galkin, Phys. Lett. B **537**, 241 (2002).
[8] H.-Y. Cheng *et al.*, Phys. Rev. D **47**, 1030 (1993).
[9] P. Colangelo, F. De Fazio, and G. Nardulli, Phys. Lett. B **316**, 555 (1993).
[10] P. Singer and G.A. Miller, Phys. Rev. D **33**, 141 (1986); Phys. Rev. D **39**, 825 (1989).
[11] J.F. Amundson, C.G. Boyd, I. Jenkins, M. Luke, A.V. Manohar, J.L. Rosner, M.J. Savage and M.B. Wise, Phys. Lett. B **296**, 415 (1992).
[12] N. Brambilla, Y. Jia, and A. Vairo, Phys. Rev. D **73**, 054005 (2006).
[13] D. Ebert, R.N. Faustov, and V.O. Galkin, Phys. Rev. D **67**, 014027 (2003).
[14] H.-M. Choi and C.-R. Ji, Phys. Rev. D **75**, 034019 (2007).
[15] W.-M. Yao *et al.* (Particle Data Group), J. Phys. G **33**, 1 (2006).
[16] H.-M. Choi and C.-R. Ji, Phys. Rev. D **72**, 013004 (2005); Phys. Rev. D **58**, 071901(R) (1998); B.L.G. Bakker, H.-M. Choi and C.-R. Ji, Phys. Rev. D **63**, 074014 (2001); Phys. Rev. D **65**, 116001 (2002); Phys. Rev. D **67**, 113007 (2003).
[17] A. Heister *et al.*, ALEPH Collaboration, Phys. Lett. B **530**, 56 (2002) and references therein.
[18] D. Becirevic *et al.*, Phys. Rev. D **60**, 074501 (1999).
[19] C. Aubin *et al.* (HPQCD Collaboration), Phys. Rev. Lett. **95**, 122002 (2005).
[20] S. Narison, Phys. Lett. B **520**, 115 (2001).
[21] G. Cvetic *et al.*, Phys. Lett. B **596**, 84 (2004); G.-L. Wang, Phys. Lett. B **633**, 492 (2006).
[22] S. Capstick and S. Godfrey, Phys. Rev. D **41**, 2856 (1990).
[23] D. Ebert, R.N. Faustov and V.O. Galkin, Phys. Lett. B **635**, 93 (2006).
[24] A. Gray *et al.* (HPQCD Collaboration), Phys. Rev. Lett. **95**, 212001 (2005).
[25] S. Hashimoto, Int. J. Mod. Phys. A **20**, 5133 (2005).
[26] M. Jamin and B.O. Lange, Phys. Rev. D **65**, 056005 (2002).
[27] M. Artuso *et al.*, CLEO Collaboration, Phys. Rev. Lett. **95**, 251801 (2005).
[28] M. Artuso *et al.*, CLEO Collaboration, Phys. Rev. Lett. **99**, 071802 (2007).
[29] K.W. Edwards *et al.*, CLEO Collaboration, Phys. Rev. Lett. **86**, 30 (2001).
[30] K. Ikado *et al.*, Belle Collaboration, Phys. Rev. Lett. **97**, 251802 (2006).
[31] S. Godfrey and J. L. Rosner, Phys. Rev. D **64**, 074011 (2001) and references therein.
[32] P. Moxhay and J.L. Rosner, Phys. Rev. D **28**, 1132 (1983); R. McClary and N. Byers, Phys. Rev. D **28**, 1692 (1983); H. Grotch, D.A. Owen, and K.J. Sebastian, Phys. Rev. D **30**, 1924 (1984); F.J. Yndurain, hep-ph/9910399; X. Zhang, K.J. Sebastian, and H. Grotch, Phys. Rev. D **44**, 1606 (1991); T.A. Lähde, C.J. Nyfält, and D.O. Riska, Nucl. Phys. A **645**, 587 (1999); Y.J. Ng, J. Pantaleone, and S.-H. H. Tye, Phys. Rev. Lett. **55**, 916 (1985); UKQCD Collaboration, L. Marcantonio *et al.*, Nucl. Phys. B (Proc. Suppl.) **94**, 363 (2001); E. Eichten and C. Quigg, Phys. Rev. D **49**, 5845 (1994).